Microfluidic chambers for monitoring leukocyte trafficking and humanized nano-proresolving medicines interactions

Caroline N. Jones[a], Jesmond Dalli[b], Laurie Dimisko[a], Elisabeth Wong[a], Charles N. Serhan[b], and Daniel Irimia[a,1]

[a]Center for Engineering in Medicine, Massachusetts General Hospital, Harvard Medical School, Shriners Hospital for Children, Boston, MA 02114; and [b]Center for Experimental Therapeutics and Reperfusion Injury, Department of Anesthesiology, Perioperative and Pain Medicine, Harvard Institutes of Medicine, Brigham and Women's Hospital and Harvard Medical School, Boston, MA 02115

Edited by David A. Weitz, Harvard University, Cambridge, MA, and approved October 19, 2012 (received for review June 19, 2012)

Leukocyte trafficking plays a critical role in determining the progress and resolution of inflammation. Although significant progress has been made in understanding the role of leukocyte activation in inflammation, dissecting the interactions between different leukocyte subpopulations during trafficking is hampered by the complexity of in vivo conditions and the lack of detail of current in vitro assays. To measure the effects of the interactions between neutrophils and monocytes migrating in response to various chemoattractants, at single-cell resolution, we developed a microfluidic platform that replicates critical features of focal inflammation sites. We integrated an elastase assay into the focal chemotactic chambers (FCCs) of our device that enabled us to distinguish between phlogistic and nonphlogistic cell recruitment. We found that lipoxin A_4 and resolvin D1, in solution or incorporated into nano–proresolving medicines, reduced neutrophil and monocyte trafficking toward leukotriene B_4. Lipoxin A_4 also reduced the elastase release from homogenous and heterogenous mixtures of neutrophils and monocytes. Surprisingly, the effect of resolvin D1 on heterogenous mixtures was antisynergistic, resulting in a transient spike in elastase activity, which was quickly terminated, and the degraded elastin removed by the leukocytes inside the FCCs. Therefore, the microfluidic assay provides a robust platform for measuring the effect of leukocyte interactions during trafficking and for characterizing the effects of inflammation mediators.

lipid mediators | therapeutics | metabolomics | chemical gradients | chemotaxis

Inflammation is a complex and finely tuned response to both infectious and noninfectious agents. The first line of defense is the innate immune system, and neutrophils are the first cells to accumulate at the site of inflammation, where they have the ability to contain invading pathogens and clear tissue debris (Fig. 1*A*). The metrics underlying these processes have been estimated using models of acute self-limited inflammation, and studies have shown that neutrophil recruitment reaches a maximum by 12 h, corresponding to the peak of inflammation. Monocytes are recruited more slowly, reaching a maximum between 24–72 h after the onset of inflammation and, in most, cases trigger the resolution phase of the inflammatory response (1, 2). Abnormal timing and dynamics of leukocyte responses are held to be the underlying causes of many inflammatory conditions, including sepsis (3), atherosclerosis (4–5), and ischemia–reperfusion injury (6). In the quest to identify and screen novel therapeutics to correct such conditions, it is critical to obtain precise measurements of both proinflammatory and proresolving processes and the underlying factors modulating leukocyte interactions.

Of increasing interest for promoting inflammation resolution is the characterization of emerging classes of lipid mediators of inflammation. These include lipoxins, resolvins, and recently developed humanized nano–proresolving medicines (NPRMs). Lipoxins are potent monocyte-specific chemoattractants but are so in a nonphlogistic manner, because they are able to activate chemotaxis of monocytes without stimulating the release of proinflammatory chemokines (7) and yet can stop polymorphonuclear neutrophil (PMN) recruitment in vivo (8, 9). Resolvins are potent mediators biosynthesized from polyunsaturated fatty acids, with each potent member sharing a defining action in resolving inflammation (7, 10–12). NPRMs were first described by Norling et al. (13) as derivations of microparticles (MPs) released from neutrophils upon activation that exert proresolving and anti-inflammatory actions (14). To augment the proresolving activities of MPs, MPs were enriched with proresolving lipid mediators to produce NPRMs (8, 15).

Toward the goal of characterizing the temporal aspects of leukocyte accumulation in conditions relevant for inflammation dynamics, several techniques have been developed to study leukocyte trafficking. In vivo imaging techniques using two-photon techniques (16), micro–single-photon emission computed tomography (17), and fluorescent cell-tracking dyes have been designed for the monitoring of labeled leukocytes during distinct stages of the inflammatory response. These assays can only provide information in a limited spatiotemporal frame, and control over the conditions at the inflammation sites is very challenging. In vivo assays, such as the mouse air-pouch model (18), peritoneal lavage (DPL) (19), or bronchoalveolar lavage (BAL) (20), provide bulk measurements for leukocytes responding to a given proinflammatory stimulus. An in vivo human model for inflammatory responses, established by Segal et al., records the accumulation of cells in cantharidin-induced skin blisters (21, 22). Temporal resolution in these studies was limited to 24-h increments, and, in general, all in vivo assays lack the resolution to capture the complex leukocyte interactions taking place during the response. For the study of human leukocyte responses, the primary systems used are classic in vitro migration assays, such as the membrane filter method. Introduced by Boyden in 1962, the filter method is an end-point assay, unable to capture the detailed dynamics of the multiple cells types involved in these responses. Microfluidic devices have emerged to avoid these shortcomings and provide novel capabilities for multiple stable gradients (23), dynamic gradient changes (24), higher throughput (25), or ease of use (26). However, none of these devices has the ability to model neutrophil and monocyte interactions while trafficking toward sites of inflammation.

Author contributions: C.N.J., J.D., C.N.S., and D.I. designed research; C.N.J., J.D., and L.D. performed research; C.N.J., J.D., C.N.S., and D.I. contributed new reagents/analytic tools; C.N.J., L.D., and E.W. analyzed data; and C.N.J., J.D., C.N.S., and D.I. wrote the paper.

Conflict of interest statement: C.N.S. is listed as an inventor on patents related to resolvins that have been assigned to Brigham and Women's Hospital and licensed to Resolvyx Pharmaceuticals. C.N.S. is a scientific founder of Resolvyx Pharmaceuticals and owns equity in the company. The interests of C.N.S. were reviewed and are managed by the Brigham and Women's Hospital and Partners HealthCare in accordance with their conflict of interest policies. The other authors declare no conflict of interest.

This article is a PNAS Direct Submission.

[1]To whom correspondence should be addressed. E-mail: dirimia@hms.harvard.edu.

This article contains supporting information online at www.pnas.org/lookup/suppl/doi:10.1073/pnas.1210269109/-/DCSupplemental.

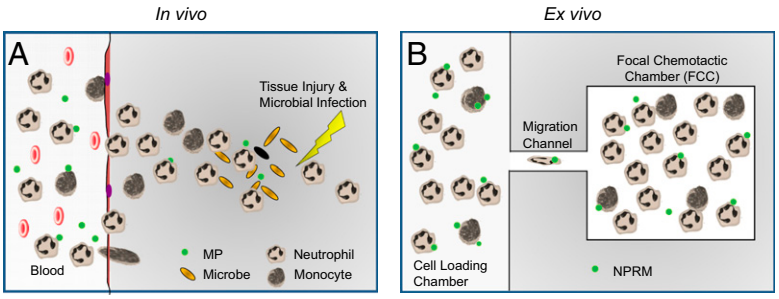

Fig. 1. Schematic of in vivo inflammation vs. in vitro microfluidic inflammation model. (*A*) After injury and microbial infection (orange grains), damaged tissue and bacteria produce gradients of chemoattractants that act as a compass for neutrophil and monocyte chemotaxis. MPs, which are neutrophil-derived, help to resolve inflammation. (*B*) Our device models inflammation and is primed with proinflammatory chemoattractants, and neutrophils and monocytes migrate and accumulate in the FCC, and their numbers can be accurately quantified. NPRMs are MPs supplemented with lipid mediators to augment proresolving activities.

To address the limitations of current techniques, we designed a microscale assay that allows real-time high-resolution measurement of human leukocyte chemotaxis in response to soluble mediators (Fig. 1*B*). We validated these devices by showing, first, that human neutrophils accumulate more rapidly than monocytes toward specific chemoattractants, in agreement with previous observations in murine models. We next used these devices to investigate direct actions of lipoxins, resolvins, and humanized NPRMs. By incorporating an elastin degradation assay into the devices, we characterized the inflammatory phenotype of the innate immune cells recruited in response to lipid mediators in vitro, showing that leukotriene (LT)B_4 and lipoxin (LX)A_4 recruit functionally distinct human monocyte, and resolvin (Rv)D1 changes the interactions between neutrophils and monocytes.

Results

Microfluidic Platform Design and Characterization. Chemoattractant gradients were established between an array of 16 focal chemotactic chambers (FCCs) at the periphery and 1 central cell loading chamber (CLC) before cells were introduced into the device. The FCC, with a volume of ~2.6 nL, simulated the inflammatory focus, whereas the central CLC served as a cell source and also acted as a sink for the chemoattractant diffusing from the FCCs (Fig. 2 *A*–*C*). As expected, neutrophils started to migrate toward the preestablished LTB_4 chemoattractant gradient source in the FCC minutes after being introduced into the CLC, and their numbers reached a plateau after 5 h (Fig. 2*D* and Movie S1). A bifurcation in the migration channel enabled us to distinguish between chemotactic and chemokinetic cell migration (Fig. 2*A*). Cells that follow the chemotactic gradients would turn at the bifurcation toward the FCC, whereas cells moving by chemokinesis would migrate in equal numbers toward the FCC and the exit channel leading outside of the device. The number of cells with directional migration toward the FCC was one order of magnitude larger than the number of cells that exited the device (9:1 ratio), confirming that we are measuring chemotactic cell migration. After the cells entered the FCC, their migration patterns changed, and cells appeared to be migrating randomly inside the FCC (chemokinesis).

To evaluate the dynamics and stability of the chemoattractant gradient developed between the FCC and the CLC, we primed the device with fluorescently labeled dextran (molecular mass, 1,000 Da) and measured the fluorescence levels over time. Linear gradients of chemoattractant are formed along the 400-μm-long, 10 × 10 μm cross-section migration channels, and last for more than 24 h after priming the FCCs with the chemoattractant (Fig. S1*A*). Biophysical modeling of chemoattractant diffusion in our device using the COMSOL simulation package shows that a chemoattractant gradients along the migration channel to the CLC are formed in less than 15 min for all chemoattractants, decrease by less than 10% at 6 h, and are still present at 24 h after the start of the experiments (Fig. S1 *B* and *C*).

Platform Validation with Neutrophils, Monocytes, and Standard Chemoattractants. We validated the assay by measuring the accumulation of neutrophils and monocytes from a 2:1 heterogeneous cell mixture, toward a panel of known chemoattractants (Fig. 3). As expected, predominantly monocytes (red) were attracted toward monocyte chemotactic protein (MCP)-1 (100 nM) (Fig. 3*A*), whereas interleukin (IL)-8 (10 nM) and *N*-formyl-methionine-leucine-phenylalanine (fMLP) (100 nM) were found to elicit selectively neutrophil (blue) chemotaxis (Fig. 3 *B* and *C*). A negligible number of cells entered the FCCs in the absence of a chemoattractant (Fig. 3*D*).

LTB_4 induced the recruitment of both monocytes and neutrophils toward the FCC, with distinct dynamics between the two cell types (Movie S2). Whereas neutrophils showed a strong and rapid response, reaching a plateau within the first 5 h, monocyte recruitment only reached a maximum after 8–9 h, and the magnitude of cell recruitment was four to five times lower (Fig. 3*E*). The differences in the accumulation dynamics between neutrophils and monocytes could be explained by the delayed activation of the monocytes, as well as differences in migration speed between the two cell types. Whereas neutrophils move through channels at 18 ± 5 μm/min (26) and could reach the FCC in less than 30 min, we estimated the monocyte velocity at

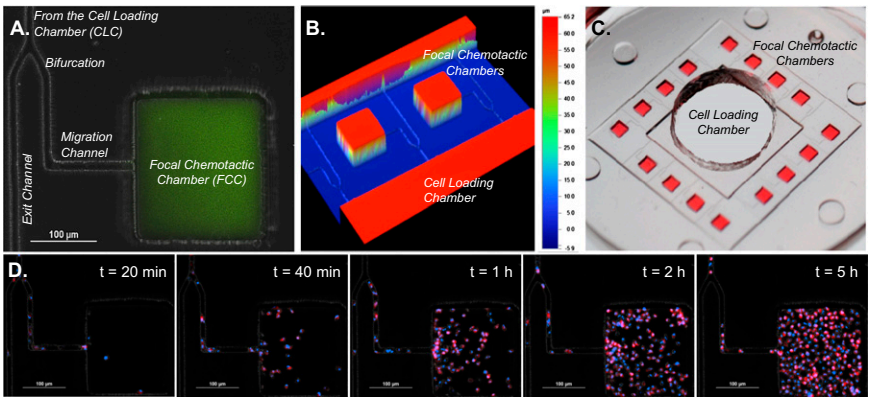

Fig. 2. Characterization of microfluidic post-diapedesis inflammation model. (*A*) Chemoattractant (green) is primed into the device and a gradient is formed along the migration channel toward the FCC. (*B*) Profilometer image of two adjacent FCCs illustrate distinct heights of FCCs and migration channels. (*C*) Large-scale model of device. (Magnification, 5×.) Sixteen FCCs (red) surround each CLC. After washing, the chemoattractant only remains in the FCC, and a linear gradient is formed along the migration channel. (*D*) Double-stained (blue, nucleus; red, membrane) neutrophils begin migrating along the LTB_4 gradient after 20 min and fill the chamber by 5 h (Movie S1).

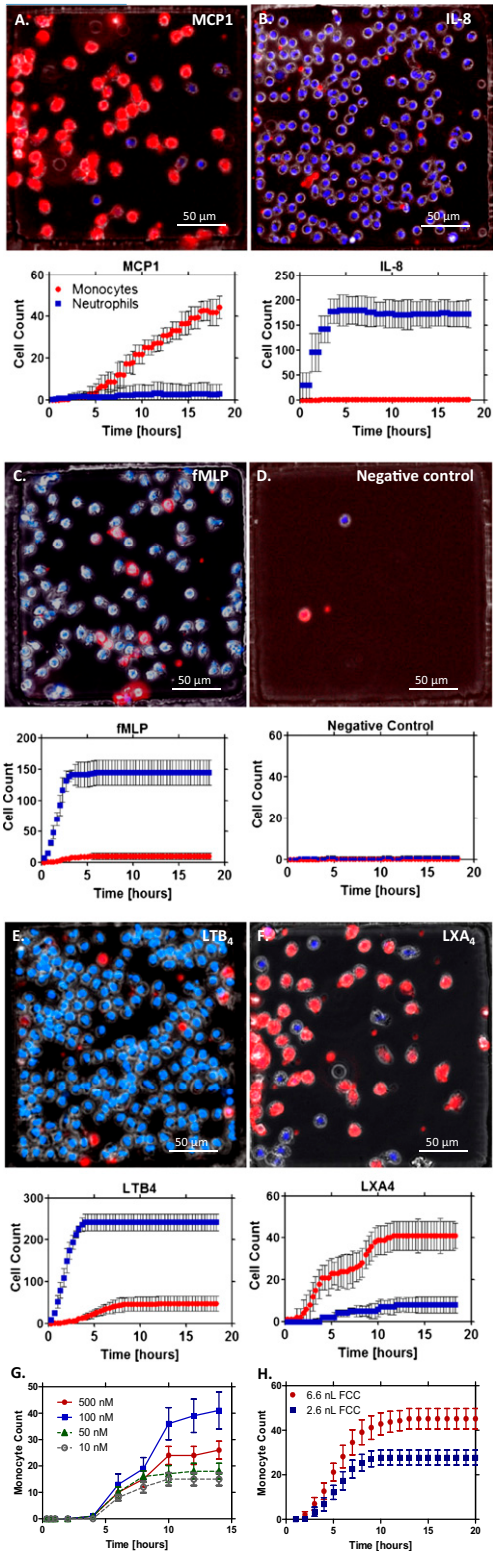

Fig. 3. Device validation. Neutrophils (blue) and monocytes (red) dynamically migrate to different chemoattractants. Graphs correspond to average cell counts in all FCCs (n = 16). (*A*–*F*) MCP-1 (100 nM) (*A*), IL-8 (10 nM) (*B*), fMLP (100 nM) (*C*), negative control (*D*), LTB_4 (100 nM) (Movie S2) (*E*), and LXA_4 (100 nM) (*F*). (*G*) Dose–response of LXA_4 as a chemoattractant to monocytes. Experiments were repeated with blood from three healthy donors for each condition. (*H*) Monocyte counts vs. time for two different-sized (6.6 vs. 2.6 nL) FCCs. The $t_{1/2}$ was ~5 h for both chambers (5 vs. 5.25), and the t_{max} occurred at 13 h (45 cells) and 9 h (28 cells) for the large and small FCCs, respectively.

5 ± 7 μm/min and calculated that monocytes would reach the FCC more than 90 min after entering the migration channels. LXA_4 induced selective monocyte recruitment that was faster and reached a plateau earlier (10 h) compared with MCP-1 (15 h; Fig. 3 *A* and *F*). Of interest, when the chemoattractant was LXA_4 , we observed two plateaus in the monocyte accumulation dynamics, suggesting the possibility that LXA_4 acts as a chemoattractant to two monocyte subpopulations that migrate at different rates. Monocyte recruitment toward LXA_4 displayed the classic bell-shaped dose-dependence characteristic for chemotaxis responses to chemoattractants, with maximal recruitment observed at the 100 nM concentration (Fig. 3*G*). We also found that chemokinesis inside the FCC stops after ~4 h in the presence of proresolving chemoattractants, such as LXA_4, whereas it continues well beyond 4 h in the presence of proinflammatory chemoattractants such as LTB_4 and fMLP. Delay time, accumulation time, and the final plateau values for both neutrophils and monocytes when migrating to the FCC in response to the panel of chemoattractants are summarized in Table S1.

To demonstrate that the final plateau number is characteristic of the cells behavior rather than an artifact of the device, we compared monocyte accumulation in the standard FCCs (2.6-nL volume) and a larger FCC (6.6 nL; large-to-small ratio, 2.5). The $t_{1/2}$ was approximately the same for both chambers (large-to-small ratio, 0.95), showing that the dynamics of cell accumulation are independent of the chamber size. The plateau number of monocytes increased with the increasing size of the chambers (large-to-small ratio, 1.7). However, the increase in monocyte number was not proportional to the size ratio, suggesting that final plateau numbers depend less on FCC volume than on cell characteristics (Fig. 3*H*).

LXA_4, RvD1, and NPRMs Significantly Reduce Monocyte and Neutrophil Chemotaxis. To quantify the modulation of monocyte trafficking in the presence of established proresolving compounds, we measured the effect of pretreatment with LXA_4 and RvD1 on the accumulation rates of monocyte toward LTB_4 as a chemoattractant (100 nM). We measured a 40% and 20% decrease in monocyte accumulation with LXA_4 and RvD1 pretreatment, respectively (Fig. 4*A*). The actions of LXA_4 appear to be proportional with the starting monocyte density in the CLC, with larger monocyte accumulation for the higher loading densities (Fig. 4*B*). We found that monocyte responses toward LTB_4 were blunted at lower seeding densities (Fig. 4*B*), and a density of 20,000 monocytes/chamber, which produced a monolayer of cells in the CLC, was determined to be optimal and was used for all of the following experiments.

We next used the trafficking platform to assess the actions of NPRMs (13), on both monocyte and neutrophil trafficking under coincubation conditions. When the leukocytes were exposed to NPRMs with a LXA_4 stable analog incorporated within their bilayers, the rate and numbers of monocyte recruitment toward an LTB_4 gradient were significantly ($P < 0.01$) reduced compared with LXA_4 alone (Fig. 4*C*). When the leukocytes were exposed to nanoparticles (NPs), which are MPs that underwent the same preparation process as NPRMs but were not enriched with proresolving lipid mediators (13), their inhibitory effect was weaker than the NPRMs. However, their inhibitory effect was still significant and likely attributable to their content of Annexin 1 (14) and is consistent with reported anti-inflammatory activity (13, 14). The average rate of cell accumulation to FCC decreased by an order of magnitude for both monocytes (down from 10 to 1 cells/h; Fig. 4*C*) and neutrophils (down from 50 to 5 cells/h; Fig. 4*D*) in the presence of NPRMs.

Heterogeneous Cell–Cell Interactions Impact Migration of Monocytes and Neutrophils. To further dissect the role of heterogenous cell–cell interactions during cell trafficking in the presence of humanized NPRM, we compared the accumulation of human neutrophils and monocyte from homogenous, as well as heterogeneous mixtures. Monocyte trafficking was enhanced under

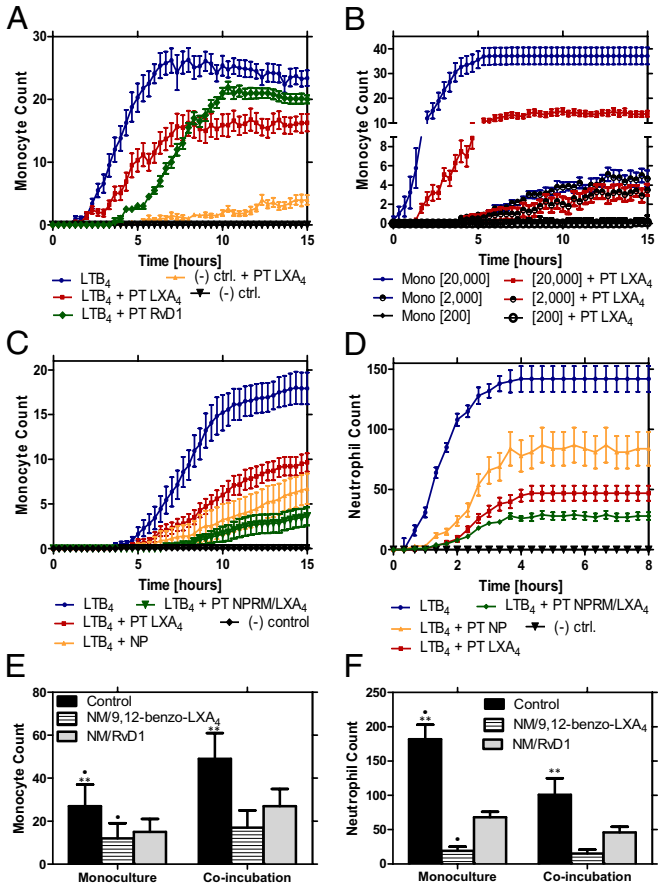

Fig. 4. Nanomedicines with 9,12-benzo-LXA_4 and RvD1 incorporated within their bilayers significantly reduce monocyte and neutrophil migration to proinflammatory chemoattractants in vitro. (*A*) Pretreatment (PT) of two known anti-inflammatory lipids, LXA_4 and RvD1, was shown to reduce monocyte migration toward LTB_4 by 40% and 20%, respectively. (*B*) Monocyte cell-seeding density was optimized ($n = 10$) to 20,000 cells/μL. At this optimal concentration, a ~60% decrease in monocyte migration was seen after pretreatment with LXA_4 (10 nM). (*C*) Dynamic counts of monocytes migrating in response to LTB_4 after pretreatment with LXA_4 (10 nM) or NPRMs with LXA_4 analog, or in the presence of NPs (MPs processed as for NPRMs but without LXA_4 enrichment) ($n = 16$). (*D*) Dynamic counts of neutrophils migrating in response to LTB_4 after pretreatment with LXA_4 (10 nM), NPRM with LXA_4 analog, or NP ($n = 16$). (*E*) Monocyte accumulation counts in response to LTB_4 control were significantly larger than after pretreatment with NPRM with LXA_4 analog and with RvD1 ($P < 0.01$). More monocytes trafficked towards LTB_4 when coincubated with neutrophils than in monoculture ($P < 0.01$). Average accumulation of monocytes isolated from three healthy donors ($n = 16$ for each donor). (*F*) In monoculture, neutrophil accumulation toward LTB_4 was significantly reduced in the presence of NPRM ($P < 0.01$). Coincubation with monocytes also reduced the neutrophil accumulation ($P < 0.01$). Average accumulation of neutrophils isolated from three healthy donors ($n = 16$ for each donor).

coincubation conditions, and NPRMs incorporating either RvD1 or a LXA_4 stable analog (9,12-benzo-LXA_4) significantly reduced monocyte trafficking toward an LTB_4 gradient ($P < 0.01$) (Fig. 4*E*). Conversely, neutrophil trafficking toward an LTB_4 gradient was reduced in coincubation conditions ($P < 0.01$) (Fig. 4*F*). Here, exposure of the neutrophils with either RvD1- or 9,12-benzo-LXA_4–containing NPRMs significantly reduced neutrophil accumulation in response to LTB_4 under both mono- and coincubation conditions. At the same time, the 9,12-benzo-LXA_4 incorporated in NPRMs was observed to be more potent at inhibiting neutrophil chemotaxis (Fig. 4*D*). Using fluorescently labeled NPRMs, we conducted real-time monitoring of these nanostructures following incubation with human monocytes. We observed that monocytes carried these nanostructure with them from the CLC into the FCC, and we observed as many as one intact NPRM to every three monocytes recorded in the FCC (Movie S3). This finding illustrates a potential mechanism of action of these nanostructures whereby migrating monocytes could redistribute the NPRMs into an inflammatory site.

Elastase Functional Assessments in Situ. To distinguish between phlogistic and nonphlogistic recruitment of monocytes, we developed a functional assay for measuring the levels of elastase produced in real time by monocytes accumulating in the nanoliter chambers. Elastase, a serine protease that hydrolyses amides and esters, is an enzyme up-regulated following phlogistic activation of monocytes (27). We validated this assay by quantifying elastase release in neutrophils, a cell type known to secrete high levels of this protein upon activation. We observed a significant increase in fluorescence levels during neutrophil recruitment toward LTB_4 (Fig. 5*A*, Movie S4, and Fig. S2*A*). During monocyte trafficking toward LTB_4, we also measured elevated elastase activity, suggestive of an activated monocyte phenotype. Elastase activity in monocytes was two orders of magnitude lower than activity detected in neutrophils and appeared to be more localized around only a subset of the monocytes recruited into the FCC (Fig. 5*B*, Movie S5, and Fig. S2*B*). A calibration curve relating fluorescence units to concentration of elastase (units per milliliter) was established with $R^2 = 0.95$ (Fig. S2*C*). In longer-duration experiments, we determined that the fluorescence loss during imaging over 10 h is less than 10% from the starting levels. A heterogeneous population of neutrophils (blue) and monocytes (bright field) migrate to LTB_4 (100 nM) and produce a relative fluorescent signal an order of magnitude less than neutrophil monoculture (Fig. 5 *C* and *D*). Monocytes attenuate neutrophil elastase production, as is known to occur in vivo (28).

When neutrophils were pretreated with RvD1, a proresolving lipid, migration to LTB_4 decreased by two-thirds (63 ± 12%), and the production per cell of elastase decreased by two orders of magnitude. Approximately half (45 ± 8%) of neutrophils stopped moving and had degraded nuclear structure after 15 h (Fig. 5*E*). Monocytes (bright field) pretreated with RvD1 migrated (44 ± 22%) less to LTB_4 and produced a third less elastase. Monocyte chemokinesis was also reduced, and monocytes stopped migrating after entering FCCs and remained in the first third of the total FCC surface (Fig. 5*F*). When a heterogeneous population of neutrophils (blue) and monocytes (bright field) migrated to LTB_4 after RvD1 pretreatment, elastase production surged almost as high as in neutrophil monoculture and then attenuated quickly after 10 h (Fig. 5 *G* and *H*).

Pretreatment with LXA_4 (100 nM) of neutrophils reduced the number of cells that migrated toward LTB_4 (100 nM) and total elastase release (Fig. 5*J*). Monocytes migrating toward LTB_4 after pretreatment with LXA_4 (100 nM) accumulated in smaller numbers and aggregated close to the entrance, in a pattern comparable to that observed for RvD1 (Fig. 5*K*). In coincubation and pretreatment with LXA_4 conditions, a smaller number of neutrophils and monocytes migrated toward the FCC, and elastase release was reduced to insignificant levels (Fig. 5 *K* and *L*).

By monitoring the localized elastase activity around monocytes accumulating in the FCC in response to LTB_4, we observed that mostly monocytes with high elastase activity arrived to the chamber during the first hours, whereas monocytes with low or no elastase activity accumulated over a longer period (Fig. 5*B*). Overall, the accumulation of two monocyte phenotypes to the FCC could be responsible for the different rates of total elastase increase over time (Fig. 5*D*). It is possible that the two monocyte phenotypes correspond with classic monocyte subpopulations defined based on surface markers and recently shown to express high levels of another serine protease, myeloperoxidase. We measured significantly lower elastase activity in monocytes when LXA_4 was the chemoattractant stimulus (79.9% lower;

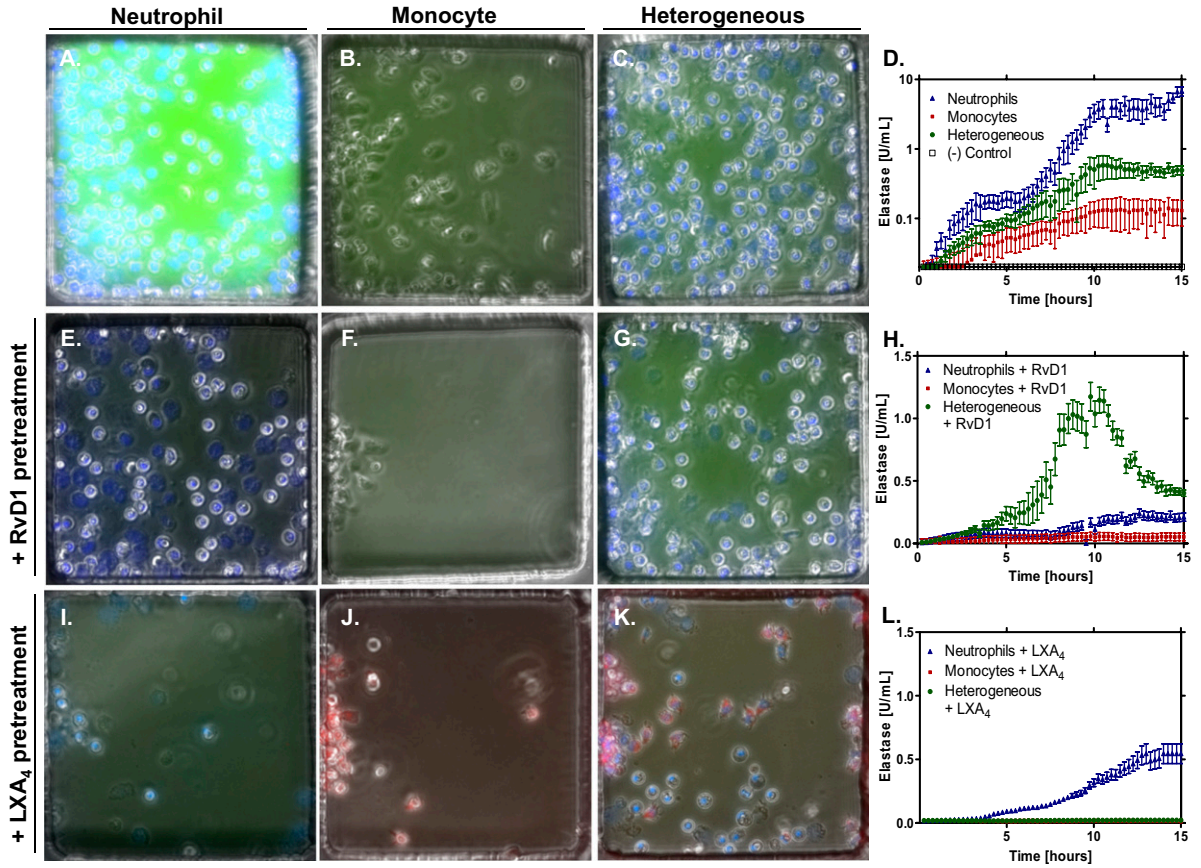

Fig. 5. Elastase assay for trafficking neutrophils and monocytes. Neutrophils (blue; *A*), monocytes (bright field; *B*), and neutrophils and monocytes (*C*) migrate to LTB_4 and produce various amounts of elastase quantified by the intensity of green fluorescence (*D*). Neutrophils alone produce two orders of magnitude more elastase than monocytes alone and one order of magnitude more elastase than a heterogeneous population of both cell types. A negative control illustrates the lack of elastase signal from a heterogeneous population of cells in the absence of a chemoattractant gradient. Neutrophils (blue; *E*), monocytes (bright field; *F*), and neutrophils and monocytes (*G*) pretreated with RvD1 (10 nM) migrate to LTB_4 and produce various amounts of elastase quantified by the intensity of green fluorescence (*H*). Pretreatment with RvD1 reduced elastase secretion by two orders of magnitude for both neutophils and monocytes. In the heterogeneous cell population, there is a transient spike of elastase secretion at the same magnitude as without RvD1 pretreatment. Neutrophils (blue; *I*), monocytes (red; *J*), and neutrophils and monocytes (*K*) pretreated with LXA_4 (10 nM) migrate to LTB_4 and produce various amounts of elastase quantified by the intensity of green fluorescence (*L*). LXA_4 pretreatment with LXA_4 reduces elastase production in all cell populations by over an order of magnitude. Results are representative of two distinct experiments (n = 18 FCCs).

$P < 0.01$) or when monocytes were pretreated with LXA_4 (10 nM) (89.3% lower; $P < 0.01$) before migration to LTB_4 (Fig. S3). The reduction in elastase activity was also significant when normalized to the number of monocytes in the chamber, suggestive for a proresolving monocyte phenotype.

Discussion

The microfluidic chambers for neutrophil and monocyte trafficking that we describe can be used to study the phlogistic and nonphlogistic recruitment and interactions between the two cell populations responding to various chemoattractants and modulators of inflammation. A key feature of the assay is the ability to probe the pro- or anti-inflammatory status of the cells trafficking toward the FCCs in the presence of lipid mediators and NPRMs. This is accomplished by the integration of a fluorescent elastase assay in each of the FCCs, which can be monitored in real time in combination with the cell trafficking. Moreover, the clearance of elastin-degradation products by phagocytic cells can be monitored and quantified as a measure of the nonphlogistic leukocyte recruitment and the resolution of the inflammation. The high sensitivity of the assay to cellular activities is the result of the favorable ratio between the total volume of the FCCs (2.6 nL) and the number of cells (tens to hundreds), as well as the minimal diffusion of the high-molecular-mass elastase and of the elastin degradation products out of the FCC.

The assay has the ability to maintain chemotactic gradients for up to 48 h, and multiple assays can be run simultaneously on standard 12- or 24-well plates. The formation of the chemotactic gradients inside the device is based entirely on diffusion from the FCCs in the absence of convection. This approach circumvents the need for external pumps (compared with other microfluidic devices) and facilitates scaling up of the assay. One potential problem in our device is that the chemoattractant gradient will change over time. A finite element model that simulates chemoattractant transport by diffusion, from the FCC through the migration channel toward the CLC, predicts that even for the small molecules such as fMLP, the gradient will decay to half of its initial slope after more than 11 h. A second concern is the steric hindrance during the simultaneous trafficking of multiple cells through the single-cell migration channel connecting the FCC to the CLC. In our experiments, we observed that faster neutrophils and monocytes can easily pass the slower cells. Previous experiments have shown that neutrophils can squeeze through 3×6 μm channels without changing their migration speed (30). Although the cross-section of the migration channels used in the current assay (10×10 μm) is five times larger, it is unlikely that neutrophils could be slowed down through a steric hindrance mechanism. Overall, we consider that the slow decay of the gradient and cell steric hindrance of the migration channels to have only minor effects on the outcome of the experiments.

The complexity of neutrophil–monocyte interactions during trafficking could not be captured using traditional chemotaxis assays. Conventional assays, such as the ubiquitous transwell devices, only provide bulk measurements of migrating cells, without single-cell resolution and are end-point assays, giving no information on the temporal course of cell accumulation. Other assays, such as the fluorescence-activated cell sorter (FACS) used to study heterogeneous cell mixtures, can only measure surface markers and cannot be used to study molecules that are secreted or other functions of the cells. Emerging microfluidic devices have also focused on traditional issues, related to either chemotaxis, cell secretion, or cell–cell interactions (31); however, our device integrates all of these aspects of cellular activity in one assay. Finally, in vivo mouse models e.g., dorsal air pouches and in vivo human model for inflammatory responses, e.g., skin blisters (21, 22) replicate the complexity of interactions. However, they have limited control over the exact conditions that cells are exposed to and have limited time resolution.

Our findings related to the trafficking and activation of leukocytes in heterogenous mixtures revealed an unexpected anti-synergistic action of RvD1. The proresolving mediator can stimulate a transient spike in neutrophil elastase activity followed by rapid degradation when neutrophils and monocytes traffic together from a heterogenous mixture in response to chemoattractant gradients. This result raises the possibility that the interactions between neutrophils and monocytes are far more complex than predicted by the current paradigm of inflammation followed by resolution controlled by the sequential arrival of neutrophils and monocytes to the inflammation sites. The elastase spike from neutrophils after coincubation and RvD1 pretreatment, being different from RvD1 pretreatment alone, is likely to be dependent on signals from the monocytes. Monocytes would also have to respond to additional activating signals from neutrophils as they distribute throughout the FCC only in the presence of neutrophils. A bidirectional communication between neutrophils and monocytes would be in agreement and could provide additional insight into the reported actions of RvD1 in vivo. For example, in mice with peritonitis, RvD1 reduces the duration and accelerates the resolution of inflammation and has an overall beneficial effect on the survival of the animals (32). Moreover, observations using the new assay show that neutrophil-derived NPRMs can reduce the number of human neutrophils and monocytes migrating in response to LTB_4, a result in agreement with their actions on murine leukocytes in vivo (13, 14). Taken together, these results suggest a bidirectional communication between neutrophils and monocytes that has not been described previously. These responses can be regulated by proresolving mediators and NPRMs and hint at approaches to regulating inflammation by modulating the interactions between neutrophils and monocytes. The microfluidic chamber device will accelerate the study of human leukocyte interactions during inflammation and will facilitate the development of mediators of resolution.

Materials and Methods

Microfluidic devices were made of PDMS bonded to glass substrates using soft lithography techniques (24). Preparation of humanized NPRMs was previously described by Norling et al. (13). Primary human neutrophil and monocyte isolation, microfluidic assay preparation and analysis, and the functional single-cell elastase assay are described in detail in *SI Text*.

ACKNOWLEDGMENTS. This work was supported, in part, by National Institutes of Health Grants DE19938 (to C.N.S. and D.I.) and GM038765 (to C.N.S.).

1. Serhan CN, Savill J (2005) Resolution of inflammation: The beginning programs the end. *Nat Immunol* 6(12):1191–1197.
2. Soehnlein O, Lindbom L (2010) Phagocyte partnership during the onset and resolution of inflammation. *Nat Rev Immunol* 10(6):427–439.
3. Perl M, Chung CS, Garber M, Huang X, Ayala A (2006) Contribution of anti-inflammatory/immune suppressive processes to the pathology of sepsis. *Front Biosci* 11:272–299.
4. Libby P (2002) Inflammation in atherosclerosis. *Nature* 420(6917):868–874.
5. Merched AJ, Ko K, Gotlinger KH, Serhan CN, Chan L (2008) Atherosclerosis: Evidence for impairment of resolution of vascular inflammation governed by specific lipid mediators. *FASEB J* 22(10):3595–3606.
6. Nathan C, Ding A (2010) Nonresolving inflammation. *Cell* 140(6):871–882.
7. Serhan CN (2007) Resolution phase of inflammation: Novel endogenous anti-inflammatory and proresolving lipid mediators and pathways. *Annu Rev Immunol* 25: 101–137.
8. Takano T, et al. (1997) Aspirin-triggered 15-epi-lipoxin A4 (LXA4) and LXA4 stable analogues are potent inhibitors of acute inflammation: Evidence for anti-inflammatory receptors. *J Exp Med* 185(9):1693–1704.
9. Maddox JF, Serhan CN (1996) Lipoxin A4 and B4 are potent stimuli for human monocyte migration and adhesion: Selective inactivation by dehydrogenation and reduction. *J Exp Med* 183(1):137–146.
10. Serhan CN, Chiang N, Van Dyke TE (2008) Resolving inflammation: Dual anti-inflammatory and pro-resolution lipid mediators. *Nat Rev Immunol* 8(5):349–361.
11. Godson C, et al. (2000) Cutting edge: Lipoxins rapidly stimulate nonphlogistic phagocytosis of apoptotic neutrophils by monocyte-derived macrophages. *J Immunol* 164(4):1663–1667.
12. Serhan CN, et al. (2003) Reduced inflammation and tissue damage in transgenic rabbits overexpressing 15-lipoxygenase and endogenous anti-inflammatory lipid mediators. *J Immunol* 171(12):6856–6865.
13. Norling LV, et al. (2011) Cutting edge: Humanized nano-proresolving medicines mimic inflammation-resolution and enhance wound healing. *J Immunol* 186(10):5543–5547.
14. Dalli J, et al. (2008) Annexin 1 mediates the rapid anti-inflammatory effects of neutrophil-derived microparticles. *Blood* 112(6):2512–2519.
15. Petasis NA, et al. (2008) Design and synthesis of benzo-lipoxin A4 analogs with enhanced stability and potent anti-inflammatory properties. *Bioorg Med Chem Lett* 18 (4):1382–1387.
16. Kreisel D, et al. (2010) In vivo two-photon imaging reveals monocyte-dependent neutrophil extravasation during pulmonary inflammation. *Proc Natl Acad Sci USA* 107 (42):18073–18078.
17. Kircher MF, et al. (2008) Noninvasive in vivo imaging of monocyte trafficking to atherosclerotic lesions. *Circulation* 117(3):388–395.
18. Romano M, *et al.* (2000) Inhibition of monocyte chemotactic protein-1 synthesis by statins. *Lab Invest* 80(7):1095–1100.
19. Henderson RB, Hobbs JA, Mathies M, Hogg N (2003) Rapid recruitment of inflammatory monocytes is independent of neutrophil migration. *Blood* 102(1): 328–335.
20. Gonzalo JA, et al. (1999) Mouse monocyte-derived chemokine is involved in airway hyperreactivity and lung inflammation. *J Immunol* 163(1):403–411.
21. Day RM, Harbord M, Forbes A, Segal AW (2001) Cantharidin blisters: A technique for investigating leukocyte trafficking and cytokine production at sites of inflammation in humans. *J Immunol Methods* 257(1-2):213–220.
22. Morris T, et al. (2010) Dichotomy in duration and severity of acute inflammatory responses in humans arising from differentially expressed proresolution pathways. *Proc Natl Acad Sci USA* 107(19):8842–8847.
23. Lin F, et al. (2005) Neutrophil migration in opposing chemoattractant gradients using microfluidic chemotaxis devices. *Ann Biomed Eng* 33(4):475–482.
24. Irimia D, et al. (2006) Microfluidic system for measuring neutrophil migratory responses to fast switches of chemical gradients. *Lab Chip* 6(2):191–198.
25. Meyvantsson I, et al. (2011) Image-based analysis of primary human neutrophil chemotaxis in an automated direct-viewing assay. *J Immunol Methods* 374(1-2):70–77.
26. Butler KL, et al. (2010) Burn injury reduces neutrophil directional migration speed in microfluidic devices. *PLoS ONE* 5(7):e11921.
27. Jones MM, Seilheimer DK, Pier GB, Rossen RD (1990) Increased elastase secretion by peripheral blood monocytes in cystic fibrosis patients. *Clin Exp Immunol* 80(3): 344–349.
28. Remold-O'Donnell E (1985) A fast-acting elastase inhibitor in human monocytes. *J Exp Med* 162(6):2142–2155.
29. Nahrendorf M, et al. (2007) The healing myocardium sequentially mobilizes two monocyte subsets with divergent and complementary functions. *J Exp Med* 204(12): 3037–3047.
30. Ambravaneswaran V, Wong IY, Aranyosi AJ, Toner M, Irimia D (2010) Directional decisions during neutrophil chemotaxis inside bifurcating channels. *Integr Biol (Camb)* 2(11-12):639–647.
31. El-Ali J, Sorger PK, Jensen KF (2006) Cells on chips. *Nature* 442(7101):403–411.
32. Chiang N, et al. (2012) Infection regulates pro-resolving mediators that lower antibiotic requirements. *Nature* 484(7395):524–528.